論文 / 著書情報
Article / Book Information

Title	Wind and Seismic Vibration Characteristics of a Tall Building Model Using Viscoelastic Damper
Authors	Daiki Sato, Kazuhiko Kasai, Tetsuro Tamura
Citation	1st International Conference on Urban Earthquake Engineering, , , pp. 485-492
Pub. date	2004, 3

WIND AND SEISMIC VIBRATION CHARACTERISTICS OF A TALL BUILDING MODEL USING VISCOELASTIC DAMPER

D. Sato[1], K. Kasai[2], and T. Tamura[3]

1) Graduate Student, Department of Built Environment, Tokyo Institute of Technology, Japan
2) Professor, Structural Engineering Research Center, Tokyo Institute of Technology, Japan
3) Professor, Department of Environmental Science and Technology, Tokyo Institute of Technology, Japan
daiki@enveng.titech.ac.jp, kasai@serc.titech.ac.jp, tamura@depe.titech.ac.jp

Abstract: This paper discusses the wind vibration control for a tall building using passive control dampers. Viscous damper and viscoelastic damper are considered in this study, and they are attached to a wind tunnel test model. The test set-up includes a special measurement system to obtain the damper hysteresis loop, which is extremely useful to understand the dynamic characteristics of the dampers and the model. Free vibration tests as well as wind vibration tests using uniform flow are conducted with or without the dampers. The model global response is correlated with the damper local response. Commonality of the damper responses obtained from the free vibration test and the wind tunnel test is discussed

1. INTRODUCTION

In Japan, most buildings may be designed against earthquake load. However they will sometimes encounter wind-related vibration discomfort of occupants, mainly due to excessive accelerations of the upper part of the tall buildings. In addition, in a case of tall building which is over 200 mm high, it is known that wind load becomes larger than earthquake load. So when the tall buildings are designed, it is necessary to consider earthquake and wind load. A number of measures to reduce the wind-induced response of those high-rise buildings were proved effective. On the aerodynamic point of view, reduction in wind forces may be achieved by configuration control to modify the structural shape. On other point, increase of building mass, stiffness, and structural damping may provide an alternative way to reduce the wind-induced response of the structure. However, increasing building mass and stiffness is expensive and may elicit larger seismic forces. It is thus more promising to increase the structural damping by employing damper devices.

In this study, either a viscous damper or a viscoelastic damper is considered as a damping device. The first application of the viscoelastic damper was made in 1969, for the World Trade Center, New York. Although thirty years have passed since the first application, the effect of the viscoelastic damper on the wind-induced response has not been fully comprehended yet. This is due to the complex nature of meteorology and wind flows, as well as sensitivity of viscoelastic material against the frequency, temperature, and strain. On the other hand, it has been recognized that the damper has significant advantage of being effective against not only the wind but also the earthquake.

While properties of viscous or viscoelastic damper are carefully considered when predicting seismic responses of the damped building, it has not been the case for wind responses. In wind engineering, the parameters such as damping ratio and vibration period are traditionally used for response prediction. In field of seismic engineering, the prediction methods of considering the damper property are already developed. Therefore this paper adopts the method to estimate for the damper

property, and will survey if such approach can be applicable to wind vibration. Pursuant to these, the present paper addresses such a study by referring to both viscous and viscoelastic dampers.

The present study uses the viscous damper of silicone oil and the viscoelastic damper, either of which is attached to a building model. The dampers are configured to suit the model, still retaining their fundamental characteristics. The test set-up includes a special measurement system to obtain the damper hysteresis loop, which is extremely useful to understand the dynamic response of the dampers and model. Free vibration tests as well as wind vibration tests are conducted with or without the dampers. The results are discussed by relating the model global response with the damper response. Regarding wind tunnel tests, uniform flow was considered and the responses due to the use of the viscous damper are explained as an example.

2. TEST MODELS

Figs. 1(a) and (b) show the test models installed with the viscoelastic dampers and viscous dampers, respectively. From now on, they will be called as "viscoelastic damper system" and "viscous damper system". A square balsa cylinder having an aspect ratio of 6 and a side ratio of 1 is used as the building model. The plan dimension and height of the square cylinder are B = 50 mm x D = 50 mm and H = 300 mm, respectively. The test model is mounted on a gimbal, and two coil springs are utilized to simulate the building stiffness in the cross-wind directions (Y-direction). The gimbal can rotate freely in the Y-direction. A laser displacement transducer is used to measure the Y-direction displacement of a point below the spring.

The viscoelastic damper (Fig. 1 (a)) is installed on same height of springs. So the viscoelastic damper has the same deformation to one spring deformation. The viscous damper (Fig. 1 (b)) is located under the displacement measurement point. Two load cells are connected to the bottom of each damper respectively, and the damper force is obtained by summing the values measured from them.

Viscoelastic damper (Fig. 1(a)) is made of the viscoelastic material (3 mm x 5 mm x 8 mm) and two aluminum plates (3 mm-thick) attached on its each side. ISD112 viscoelastic material (Sumitomo-3M Company) is used. When the building model vibrates, the relative motion between the two plates causes material deformation, reaction force, and consequently energy dissipation. The viscous damper (Fig. 1(b)) consists of the lever arm with an end plate, and silicon oil filled in a container. The end plate is sunk in the oil, and its in-plane motion causes shearing resistance of the oil and energy dissipation.

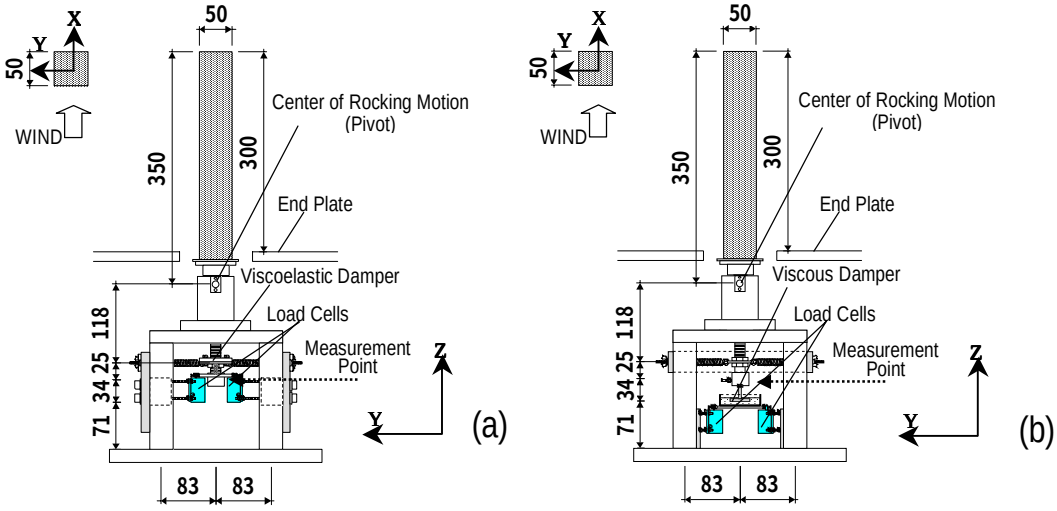

Figure 1 Test models (unit:mm): (a) Viscoelastic damper system, and (b) Viscous damper system

3. FREE VIBRATION TESTS

Free vibration tests are conducted with or without the dampers before each set of wind tunnel test. Regarding the model without the damper, the natural frequency f_0 =17.80 Hz and the damping ratio h_0 = 0.20 % are estimated from the successive peaks of the displacement time history during free vibration. As for the model with the damper, the equivalent frequency f_{eq} and the equivalent damping ratio h_{eq} are also estimated using the same method as mentioned above. After each set of wind tunnel test, free vibration tests are conducted again to verify whether there is no damage to the system.

Damping ratio of the viscoelastic damper system is adjusted by changing the temperature of the viscoelastic damper: the material becomes softer and dissipates less energy under higher temperature. Temperature of viscoelastic damper is monitored using the infrared radiation thermometer, and the light bulbs are used to control temperature of viscoelastic. Damping ratio of the viscous damper system is adjusted by changing the amount of the silicon oil.

Figs. 2(a) and (b) show examples of the damper force F_d vs. the damper deformation u_d curves, i.e., hysteresis loops of the viscous and viscoelastic dampers, respectively. They are obtained from the free vibration tests, and the viscoelastic damper's loop has clear inclination (stiffness) compared with viscous damper's loop. Thus, viscoelastic damper adds not only energy dissipation but also the stiffness to the system.

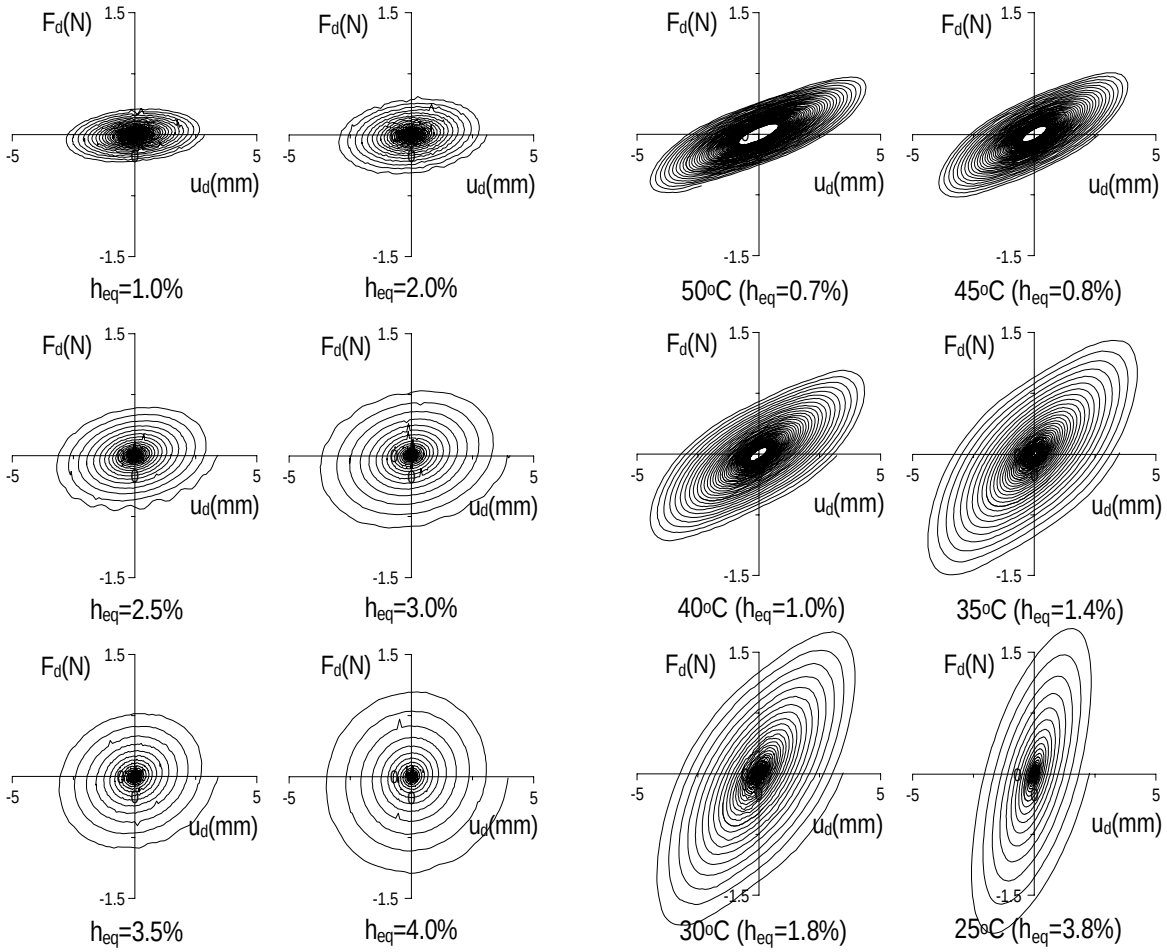

(a) Viscous Damper

(b) Viscoelastic Damper

Figure 2 Results of Free Vibration Tests

To consider the effect of the damper on the system precisely, we developed a method to obtain the equivalent frequency of the system f_{eq}' and the equivalent damping ratio of the system h_{eq}', by using the hysteresis loops of the damper. The procedure is as follows:

A hysteresis loop of the viscous and/or viscoelastic damper when undergoing steady-state response is shown in Fig. 3. The mechanical property of the damper is expressed by K_d' and η_d, the former is a storage modulus representing the stiffness (loop inclination) and the latter a loss factor representing the energy dissipation capability (loop thickness) (Kasai,.K., Okuma, K. 2001).

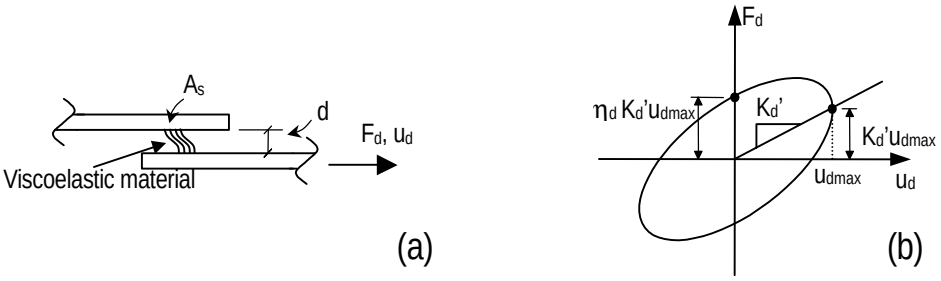

Figure 3 (a) Deformation of the Viscoelastic Damper, and (b) Force-Deformation Hysteresis Loop

K_d' and η_d can be written as in Eqs. 1a and b, using the experimental values $F_d^{(j)}$ and $u_d^{(j)}$ at the j-th step (Kasai, K., Ooki, Y., Amemiya, K., Kimura, K. 2003).

$$K_d' = \frac{n\sum F_d^{(j)} u_d^{(j)} - \sum F_d^{(j)} \sum u_d^{(j)}}{n\sum \left(u_d^{(j)}\right)^2 - \left(\sum u_d^{(j)}\right)^2}, \quad \eta_d = \frac{2E_D'}{\pi K_d' \left(u_{d\max}\right)^2} \qquad \text{(1a, b)}$$

where Σ means sum of "n" sets of $F_d^{(j)}$ and $u_d^{(j)}$ per one cycle of the hysteresis loop. E_D' is the energy dissipated by the damper per half cycle, and it is calculated from the area of the damper hysteresis loop.

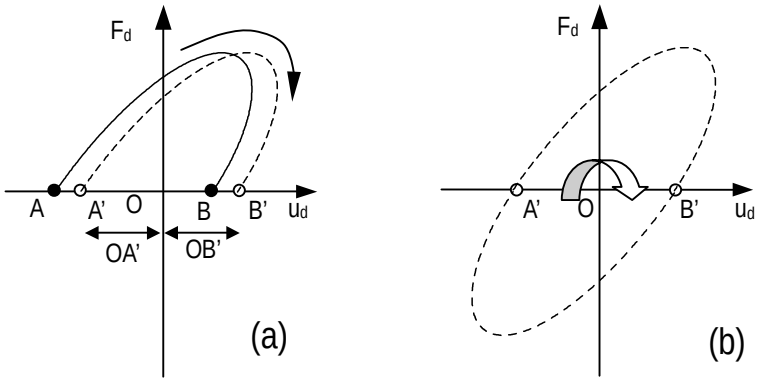

Figure 4 (a) Half Cycle, and (b) Obtained Closed Hysteresis Loop

In case of the free vibration tests, the damper force and deformation decrease in subsequent cycles, and the hysteresis loop is not necessarily closed. Thus, as shown by the solid curve in Fig. 4(a), $\overline{OA}$ is longer than $\overline{OB}$, and a large calculation error appears when using Eq. (1a) and (1b) without alteration. In order to obtain a closed hysteresis loop, the solid curve is moved along horizontal axis so that $\overline{OA}' = \overline{OB}'$ (dashed curve, Fig. 4(a)), and rotated 180^0 about the origin "O" (Fig. 4(b)).

After evaluating K_d' and η_d, the equivalent storage modulus K_{eq}' and the equivalent loss factor η_{eq} of the damped system can be calculated using following equations.

$$K_{eq}^{'} = K_s + K_d^{'}\left(\frac{L_2}{L_1}\right)^2, \quad \eta_{eq} = \frac{\eta_d}{1+(K_s / K_d^{'})(L_1 / L_2)^2} \tag{2a, b}$$

where K_S = sum of the Y-direction stiffness of the two coil springs, L_1 = distance from the pivot point to the coil springs, and L_2 = distance from the pivot point to the damper. In the present set-up, K_s = 9.42 N/mm, L_1 = 118 mm and L_2 = 118 mm (Viscoelastic damper system), = 177 mm (viscous damper system), respectively.

The equivalent frequency of system f_{eq}' and equivalent damping ratio of system h_{eq}' can be expressed as follows:

$$f_{eq}^{'} = \frac{1}{2\pi}\sqrt{\frac{K_{eq}^{'}}{M_{eff}}}, \quad h_{eq}^{'} = h_0 + \frac{\eta_{eq}}{2} \tag{3a, b}$$

where M_{eff} = effective mass at the point of coil spring, and it is estimated from the free vibration tests without damper, *i.e.*, $M_{eff} = K_s / (2\pi f_0)^2$.

The above relationship is commonly used for both viscous and viscoelastic damper systems. The coefficient of viscosity C_d, often used to express the property of a viscous damper, can be written as follows:

$$C_d = \frac{\eta_d K_d^{'}}{2\pi f_{eq}^{'}} \tag{4}$$

The errors f_{eq}' / f_{eq} and h_{eq}' / h_{eq} are shown in Fig. 5. As defined earlier, f_{eq} and h_{eq} are the equivalent frequency and damping ratio evaluated from the displacement time history of the test model, and f_{eq}' and h_{eq}' are those calculated from the damper hysteresis loop recorded (Fig. 2) as well as Eqs. 1 to 3. As shown in Fig. 5, f_{eq}' and h_{eq}' agree well with f_{eq} and h_{eq}, respectively, validating both the measurement system and the proposed evaluation method.

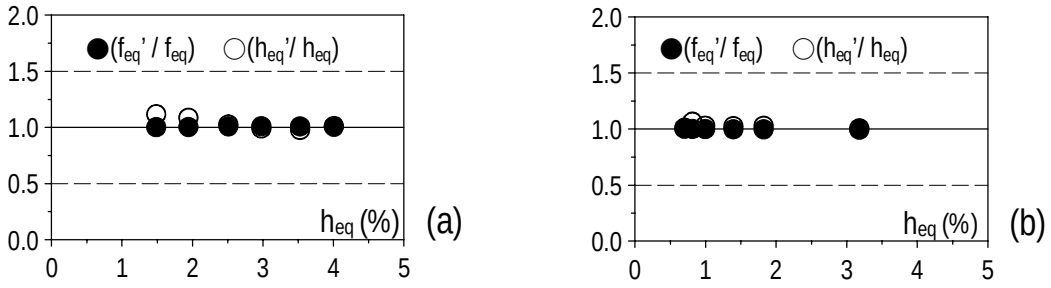

Figure 5 Error plots (a) Viscous damper system, (b) Viscoelastic damper system

4. WIND TUNNEL TEST SET UP

Wind tunnel tests are performed using the Eiffel type wind tunnel at Tokyo Institute of Technology. The cross section and length of the test section are 1000 mm x 800 mm and 7000 mm, respectively. The contraction ratio is 5 and the maximum wind speed is 25 m/s. Schematic diagram of the test set-up is shown in Fig. 6. For avoiding various noises, support structure is made very stiff and the base very heavy, thereby preventing their high-frequency vibration. The end plate is installed to reduce the effect of boundary layer on the generated uniform flows. Fig. 7(a) shows an example for the vertical distribution of U / U_H measured, where U = mean wind velocity at each elevation, and U_H= mean velocity at top of the model. The U / U_H appears to be 1.0 throughout the height of the

model. Also, Fig. 7(b) shows the vertical distribution of the turbulent intensity that was measured at the center of the turn table (Fig. 6). The boundary layer, defined to have the turbulent intensity of more than 0.3%, is located at the bottom of the model, and its depth is about 50mm, very small compared with the model height. As these indicate, the set-up accurately produces the uniform flow condition.

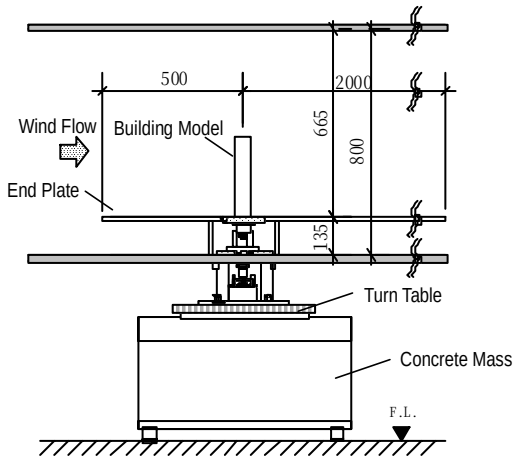

Figure 6 Schematic of the test setup in the wind tunnel. (unit:mm)

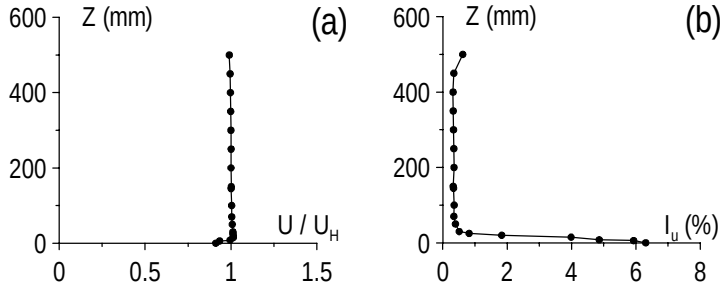

Figure 7 Vertical profile :
(a) Normalized mean velocity, and (b) Turbulent intensity

5. WIND TUNNEL TEST RESULTS

5.1 Viscous Damper System

Wind tunnel tests of the viscous damper system are performed as the first step in this study. It is general methods to use silicon oil as the damping device of the wind tunnel.

The root-mean-square (RMS) of the displacement at the measurement point (Fig. 1), namely, y_{rms} is obtained experimentally. Fig. 8 shows the RMS of the rotational angle θ_{rms} (= y_{rms} / L_1) against the reduced wind velocity V_r for various magnitudes of mass-damping parameter δ of the viscous damper system. Note that V_r = U_H /(f_0 B), where B = width of the model. Also, δ can be expressed as follows (Amano 1995):

$$\delta = \frac{\tilde{M}}{\rho B^2 L_0} h_{eq} = \frac{K_s L_1^2}{\rho (2\pi f_0)^2 B^2 L_0^3} h_{eq} \tag{5}$$

Where, $\tilde{M}$ = generalized mass, ρ = air density, L_0 = distance from the pivot point to the top of the model, 350mm. The parameter δ is adjusted by changing only the damping ratio h_{eq} as estimated from free vibration tests. The relation between δ and h_{eq} is indicated in Table 1. When δ = 0.64 (h_{eq} = 0.8 %), the peak of θ_{rms} is observed at V_r = 10.4. As δ is increased, the peak occurred at smaller V_r , and for instance, when δ = 1.04 (h_{eq} = 1.3 %), the peak occurred at V_r = 9.65. Besides, the resonant vibration is suppressed as δ was increased to 1.12 (h_{eq} = 1.4 %). The results agree well with those reported by Tamura et al. (2000).

Table 1 Relation between δ and h_{eq}

δ	0.64	0.72	0.80	0.88	0.96	1.04	1.12	1.28	1.44	1.60
h_{eq} (%)	0.8	0.9	1.0	1.1	1.2	1.3	1.4	1.6	1.8	2.0

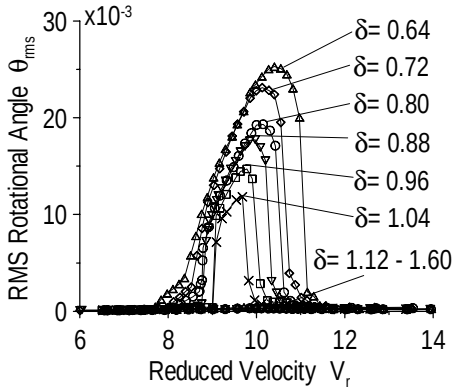

Figure 8 RMS response curve in the viscous damper system

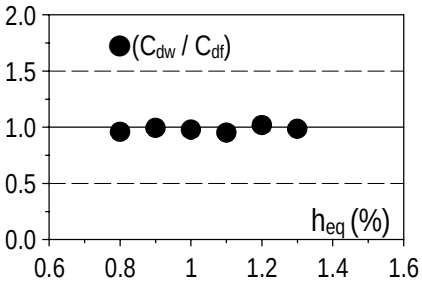

Figure 10 Comparison between C_{dw} and C_{df}

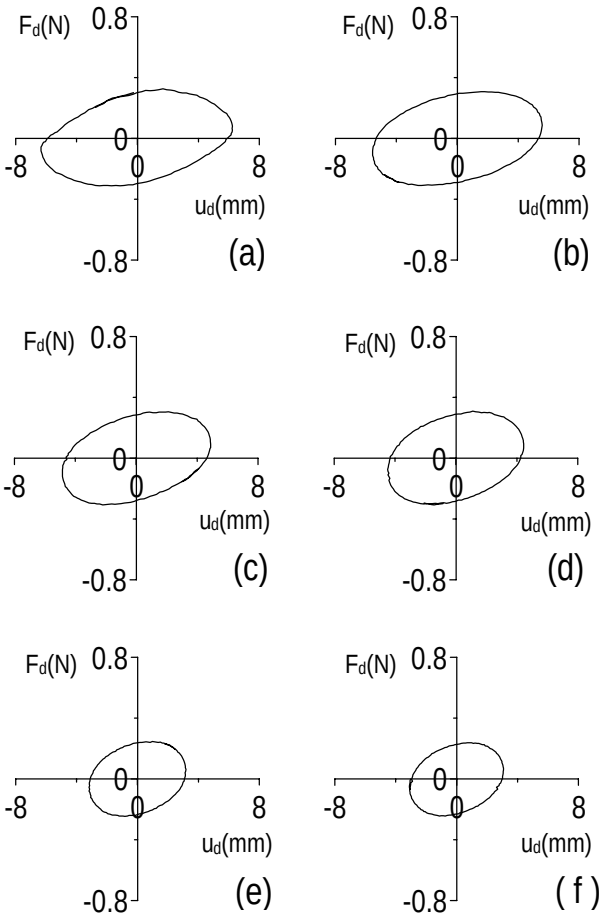

Figure 9 Damper hysteresis loops in wind tunnel tests: (a) δ=0.64, (b) δ=0.72, (c) δ=0.80, (d) δ=0.88, (e) δ=0.96, (f) δ=1.04

Fig. 9 shows the damper hysteresis loops recorded when RMS rotational angle was at peak. Plots of ratios C_{dw} / C_{df} are also shown in Fig. 10, where C_{df} and C_{dw} = coefficients of damper viscosity estimated from the damper hysteresis loops recorded during the free vibration test and wind tunnel test, respectively. Note that the latter was calculated from the loops at the resonance state (Fig. 8), and the alteration such as shown in Fig. 4 was not needed. As in Fig. 10, C_{df} coincides well with C_{dw}, confirming that the resonance response under uniform flow can be characterized by the property of the damper obtained from the free vibration test. In addition to this, the measurement system has made it possible to correlate the responses of the model and the damper.

5.2 Comparison with Viscous Damper System and Viscoelastic Damper System

Wind tunnel tests of the viscoelastic damper system are carried out under same damping ratio heq case of the viscose damper system. The damping ratio of the viscoelastic damper system is obtained from the free vibration test in which is carried out before the wind tunnel test, and then the viscoelastic damper temperature, which is monitored by thermometer, is decided. During wind tunnel test, the temperature is controlled adjusting the brightness of the light bulb, as maintained uniformly.

Comparing the wind tunnel test results of the viscous damper system and the viscoelastic damper system are shown in Figs. 11 (a) and (b). The result in the case of δ = 0.64 is shown in Fig. 11 (a), and the result in the case of δ = 0.72 is shown in Fig. 11 (b). As in Fig. 11, the value θ_{rms} at peak are similar the viscose damper system and the viscoelastic damper system, but Vr when peak θ_{rms} occurs. In case of the viscoelastic damper system, peak θ_{rms} occurs at higher Vr compare in case of viscose damper system.

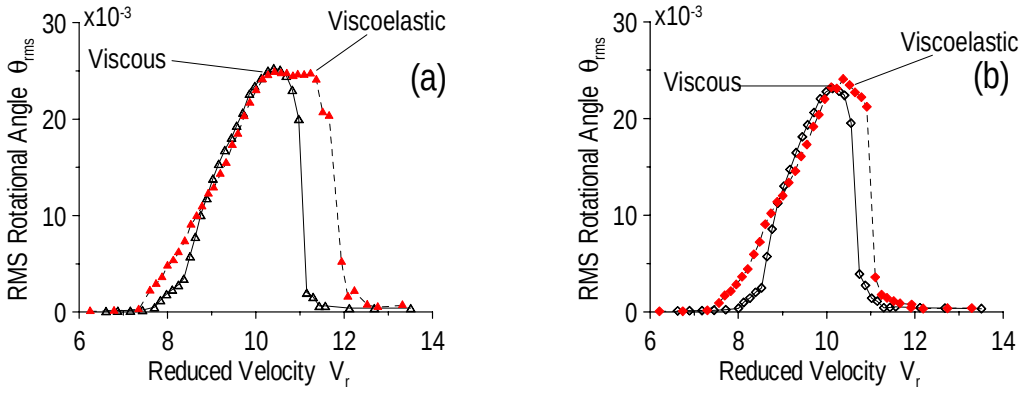

Figure 11 Comparison with the viscous damper system and the viscoelastic damper system :

(a) δ = 0.64, (b) δ = 0.72

6. CONCLUSION

This paper has discussed the first step of our study on wind vibration control for a tall building using passive control dampers. The objective of this study is to evaluate the wind response reduction scheme by considering significantly different characteristics of various dampers available in Japan. Viscous damper and the viscoelastic damper are considered in this study, and they are attached to a wind tunnel test model. A special measurement system was created to obtain the relationship between local damper force and deformation, essential information towards a comprehensive study on building global responses. The conclusions are as follows:

(1) Hysteresis loops of the dampers recorded during the free vibration tests clearly indicate different dynamic properties of the viscous damper and viscoelastic damper. The proposed method to estimate the damper storage modulus and the loss factor from the loops appears to be very reliable.
(2) Equivalent frequency and equivalent damping ratio of the damped building model can be estimated from the above-mentioned damper storage modulus and the loss factor, and they appear to agree well with those evaluated from the global displacement time history of the model subjected to free vibration.
(3) The coefficients of the damper viscosity estimated from the free vibration tests and from the wind tunnel tests agreed well. Thus, the resonance response under uniform flow can be characterized by the property of the damper obtained from the free vibration test. Moreover, the measurement system has made it possible to correlate the responses of the model and the damper.
(4) The viscoelastic system showed the peak RMS rotational angle at a higher value than the viscous damper system.

References:

Kasai, K., Okuma, K. (2001), "Kelvin-Type Formulation and Its Accuracy for Practical Modeling of Linear Viscoelastic Dampers," (Part 1 One-mass system having damper and elastic/inelastic frame), *Journal of Structural and Construction Engineering*, No. 550, 71-78

Kasai, K., Ooki, Y., Amemiya, K., Katuhiko, K. (2003), "A constitutive rule for viscoelastic materials materials combining ISO-butylene and stylene polymers," (Part 1 Liner model considering temperature and frequency sensitivities), *Journal of Structural and Construction Engineering*, No. 569, 47-54

Amano, T. (1995), "The Effect of Corner-Cutting of Three-Dimensional Square Cylinders on Vortex-Induced Oscillation and Galloping in Uniform Flows," *Journal of Structural and Construction Engineering*, No. 478, 63-69

Tamura, T., Okada, R., Wada, A. (2000), "Wind Tunnel Test on Dynamic Behavior Near Resonant Region for High-Rise Building Model With Hysteretic Damper," *Journal of Structural and Construction Engineering*, No. 537, pp.35-41